Supplementary Information

Material and Methods

Materials

Lyophilized L-α-phosphatidylcholine from soybean was purchased from Sigma-Aldrich. $C_{12}E_8$ was bought from Nikko Chemicals Co., LTD. Japan. $[Cu(CH_3CN)_4]PF_6$, AMPPCP, and L-cysteine were obtained from Sigma-Aldrich.

Cloning and mutagenesis of LpCopA mutants

Primer design and plasmids (pET22(+)) of the LpCopA mutants (M148V, D426N, C382A, C384A, C384S, C382S C384S, C382S C384S M717A, C18S C42S C56S C59S, Y688F, N689A, S721A) were prepared by site-directed mutagenesis using QuikChange® from Agilent Technologies.

The heavy metal binding domain of LpCopA (residues 1 to 84, with an additional alanine in position 2) was cloned from the wild-type LpCopA [1] by the use of the forward primer sequence GCC CAT ATG GCT AAA CAC GAC CAC and the reverse primer sequence GCCC GC GGC CGC TTA TCG ACG TCT CAT ATC AAG ATA TTC and cloned into the pET22(+) vector.

Sample preparation of wtLpCopA and mutants

Protein expression, membrane preparation and the affinity chromatography with Ni-NTA for wtLpCopA, mutants, and ΔHMBDLpCopA (residues 1 to 73 are missing) were performed as previously described with one slight modification [1], as the protein was directly transferred to Buffer E [20 mM MOPS-KOH pH=6.8, 80 mM KCl, 20% glycerol, 5 mM β-mercaptoethanol (BME), 1 mM $MgCl_2$ and 0.28 mM $C_{12}E_8$] using a PD-10 desalting column (GE Healthcare) instead of a Superose 6 column. Typically, the mutants were concentrated to 5 to 10 mg/ml (Vivaspin, 50 kDa cutoff), flash frozen in 250 µl aliquots and stored at -80°C until further use.

Protein purity and amount was checked by SDS-PAGE. Monodispersity of the mutant forms compared to wt protein was analyzed by a Superose 6 column (CV 24 ml). Protein of comparable monodispersity to the wt was utilized for all subsequent experiments.

Protein concentration was estimated from the absorption at 280 nm using a NanoDrop ND-1000 spectrophotometer (Thermo Scientifc), using an extinction coefficient of 59930 M^{-1} cm^{-1} for wtLpCopA and the mutants, while an extinction coefficient of 58440 M^{-1} cm^{-1} was used for the ΔHMBD LpCopA.

HMBD expression and purification

Recombinant HMBD of LpCopA was expressed in *E. coli* BL21 (DE3) GOLD cells. Transformed cells were grown at 37 °C in TB-Glycerol media containing 50 mg/l ampicillin until an OD_{600} = 1 was reached, cooled at 30 °C and protein expression was induced by addition of 1 mM isopropyl β-D-1-thiogalactopyranoside (IPTG). Cells were harvested after 4 h post-induction by centrifugation (9000g, 4 °C, 20 min) and cell pellets were stored at -80 °C until further use. Cells were suspended in 20 mM Tris-HCl pH = 8, 500 mM NaCl, 5mM $MgCl_2$, 1 mM DTT supplemented with 30 g/ml of DNaseI from bovine pancreas (Sigma-Aldrich) and EDTA-free protease inhibitor cocktail (Roche) to a final concentration of 0.1 g cells/ml. Typically 20 g cells were disrupted by 3-pass cycles in a microfluidizer operating at a pressure of 18000-20000 psi. Cell debris was removed by centrifugation (15900g, 4°C, 30 min). Supernatant was collected and buffer composition subsequently adjusted to 20 mM Tris-HCl pH=8, 500 mM NaCl, 5 mM $MgCl_2$, 1 mM DTT and 25 mM imidazole. The protein was purified by affinity chromatography upon supernatant incubation with 5 ml Ni-NTA beads for 2 h at 4 °C under stirring. Resin was loaded on a gravity column and beads washed with 30 column volumes of 20 mM Tris-HCl pH = 8, 500 mM NaCl, 25 mM imidazole, 1 mM DTT and protein eluted in 20 mM Tris-HCl pH=8, 250 mM NaCl, 250 mM imidazole, 1 mM DTT. Protein containing fractions were pooled and further purified by size-exclusion chromatography with a Superdex 75 10/30 column eluted with 20 mM Tris-HCl pH=8, 250 mM NaCl, 1 mM DTT, 1 mM EDTA. The peak corresponding to monomeric protein was collected, flash frozen in liquid N_2 and stored at -80 °C. Protein concentration was determined by absorption spectroscopy using an extinction coefficient of 2980 M^{-1} cm^{-1}.

Determination of Cu^+ binding stoichiometry

Protein stocks and all solutions were made oxygen-free on a Schlenk-line via eight vacuum-argon cycles. Sample preparation was performed in an argon (90%)-hydrogen (10%) purged Coy anaerobic chamber equipped with palladium catalyst cassettes for removal of residual molecular oxygen. All buffers and stock solutions were treated with Chelex-100 resin before use to remove metal traces.

Protein stocks were diluted into Buffer E and the buffer was exchanged to a final Buffer E without BME. Additionally, to a subset of the LpCopA variants, final concentrations of 20 mM cysteine and 1 mM nucleotide were prepared. Copper binding was achieved by addition to the protein of an excess (6 Cu^+ eq.) of a freshly prepared stock solution of $[Cu(CH_3CN)_4]PF_6$ dissolved in CH_3CN. Free or loosely bound metal was removed using a 5 ml Hi Trap desalting column packed with Sephadex G-25 resin (GE Healthcare, USA). Cu^+ content was determined by ICP-MS as indicated below. Protein concentration was estimated by absorption spectroscopy at 280 nm and independently using a Bradford assay in 96-well plate format using bovine serum albumin as a standard. 96-well plate absorbance measurements at 595 nm were performed on a Tecan Infinite M200 instrument.

Determination of Cu^+ stoichiometry to the isolated HMBD was performed on samples prepared for XAS measurements.

XAS sample preparation

All buffers and stock solutions were treated with Chelex-100 resin before use to remove metal traces. HMBD of LpCopA, wt and ΔHMBD LpCopA samples and stock solutions for XAS were rendered oxygen-free on a Schlenk line and all sample preparation steps were performed in an argon (90%)-hydrogen (10%) purged glove-box equipped with palladium catalyst cassettes. Two different reconstitution procedures were undertaken for wt/ΔHMBD LpCopA and HMBD.

Wt and ΔHMBD LpCopA stocks (approx. 20 mg/ml) were diluted 50 times in 20 mM Tris-HCl pH=7.6, 200 mM KCl, 1 mM $MgCl_2$, 0.15 mg/ml $C_{12}E_8$, 20 %(w/v) glycerol, and copper reconstitution performed by addition of a freshly prepared stock solution of $[Cu(CH_3CN)_4]PF_6$ dissolved in CH_3CN at the final Cu^+:protein stoichiometry (1:1, 1:2 for ΔHMBD, and 1:1 and 1:4 for

wtLpCopA). Samples were subsequently concentrated using Amicon-Ultra 50 kDa cutoff membrane concentrators to a final concentration of 0.4 - 0.6 mM.
The HMBD reconstitution was performed in an oxygen-free glovebox by apo-protein preparation via acid treatment to remove residual zinc bound to the protein through the expression and purification, as determined by ICP-MS analysis. An HMBD stock solution (~150 μM) was acidified to pH = 1-2 by addition of a 1 M HCl stock and immediately desalted using a 5 ml Hi-Trap desalting column packed with Sephadex G-25 resin (GE Healthcare, USA) eluted with 10 mM HCl. Copper reconstitution was performed by addition of a freshly prepared stock solution of $[Cu(CH_3CN)_4]PF_6$ dissolved in CH_3CN at the final desired Cu^+:protein stoichiometry (1:1 and 1:2) and buffer adjusted to final 50 mM Tris-HCl pH=8, 250 mM NaCl. Samples were subsequently concentrated using Amicon-Ultra 3 kDa cutoff membrane concentrators. Final metal-to-protein ratios were determined by ICP-MS upon metal release as reported below.

XAS data collection and analysis

Samples were loaded into custom-made polycarbonate XAS sample cells sealed with metal-free tape in the anaerobic glove box, flash frozen in liquid nitrogen and stored in liquid nitrogen until data collection. X-ray absorption spectroscopy measurements were performed at the Stanford Synchrotron Radiation Laboratory with the SPEAR-3 storage ring operating at 350 mA at 3.0 GeV. Copper K-edge data were collected using beamline 7-3 with a wiggler field of 2 Teslas and employing an Si(220) double-crystal monochromator and a vertically-collimating pre-monochromator harmonic rejection mirror. The incident and transmitted X-ray intensities were monitored using nitrogen-filled ionization chambers, and X-ray absorption was measured as the copper Kα fluorescence using an array of 30 germanium detectors. Nickel filters were placed between the cryostat and detector to reduce scattered X-ray not associated with copper fluorescence. During data collection, samples were maintained at a temperature of ~10 K using an Oxford Instruments liquid helium flow cryostat. XAS spectra were measured using 10- eV step in the pre-edge region (8750–8960 eV), 0.35 eV steps in the edge region (8960–9010 eV) and 0.05 $Å^{-1}$ increments in the EXAFS

region (to k = 13.1 $Å^{-1}$). Two to five ~40-min scans were accumulated, and the energy was calibrated by reference to the absorption of a standard copper metal foil measured simultaneously with each scan, assuming a lowest energy inflection point of the copper foil to be 8980.3 eV.

The EXAFS oscillations (k) were quantitatively analyzed by curve fitting using the EXAFSPAK suite (George, G.N., EXAFSPAK, http://ssrl.slac.stanford.edu/exafspak.html). *Ab initio* theoretical phase and amplitude functions were calculated using the program FEFF version 8.2 [2]. Data obtained from each Ge-detector element were checked for spectral anomalies and data from elements showing abnormal responses were excluded from data averaging. No smoothing, filtering, or related operations were performed on the data.

ICP-MS analysis

For ICP-MS, protein samples were mixed with concentrated HNO_3 (69 %(w/v)) to obtain a HNO_3 concentration of 10 %(w/v), and digested at 80 °C for 2 h - 16 h hours. Samples were subsequently diluted to a final concentration of 1 %(w/v) HNO_3. ICP-MS has been performed on a Hewlett-Packard 4500 ICP mass spectrometer (Agilent Technologies, Caltech Environmental Analysis Center) connected to CETAC ASX-500 auto-sampler for sample injection. The corresponding buffers have been used for background blank subtraction. High-purity TraceSelect nitric acid, $CuCl_2$ standard solutions and TraceSelect H_2O were from Sigma-Aldrich.

ATP hydrolysis assay

ATPase activity in a lipid-detergent solution environment was measured by a modified colorimetric phosphate detection method introduced by Baginski with bismuth detection under aerobic conditions[3] in a 96-well plate.

wtLpCopA (15 µg, 4 µM final concentration), or one of the mutants, was mixed with reaction buffer [40 mM MOPS-KOH pH = 6.8, 150 mM NaCl, 5 mM KCl, 5 mM $MgCl_2$, 20 mM $(NH_4)_2$ SO_4, 1.2 mg/ml L-α-phosphatidylcholine, 3 mg/ml $C_{12}E_8$, 20 mM L-cysteine, 5 mM NaN_3, 0.25 mM Na_2MoO_4, 0.01 mM $[NH_4]_2MoS_4$] in a total volume of 50 µl. Either 1 µl of 25 mM $CuCl_2$ (0.5 mM final concentration) or 5 µl of a 10x stock of different $CuCl_2$ concentrations

from a dilution series (0 and 20 mM) was added. The reaction was initiated by the addition of a 10x stock of different ATP concentrations from a dilution series (0 to 100 mM) in the case of a fixed concentration of $CuCl_2$ (0.5 mM) in the reaction mixture, or by 2 µl of 125 mM ATP (5 mM final concentration) in the case of the $CuCl_2$ concentration variation. The reaction was incubated for 30 min at 37 °C and stopped by the addition of 75 µl of freshly prepared development solution (2.86 %(w/v) ascorbic acid, 1 M HCl, 0.48 %(w/v) $(NH_4)_2MoO_4$, 2.86 %(w/v) SDS). The color development was stopped with 125 µl of stop solution (3.5 %(w/v) bismuth citrate, 3.5%(w/v) sodium citrate, 1 M HCl) and the absorption was measured at 710 nm on a VICTOR 3 1420 Multilabel Plate Reader (PerkinElmer). At least three independent measurements for each condition were performed. For a phosphate (P_i) standard curve, increasing KH_2PO_4 concentrations (0 to 0.4 mM) were measured in triplicates on each plate with a total volume of 50 µl.

Statistical analysis of ATPase activity

Statistical analysis was performed using KaleidaGraph v4.1.3 for MacOSx (Synergy Software). Cu^+/ATP independent background activity was subtracted from the 0 mM $CuCl_2$/ATP values.

Specific ATPase activity was calculated by the use of equation 1:

$$v = \frac{Abs_{710}}{m_{P_i} * c * t} \quad (1)$$

Where *v* corresponds to the specific activity given in nmol P_i/mg protein/min, Abs_{710} is the background-corrected measured absorption, m_{pi} allocates the slope of the phosphate standard curve in µM, *c* is the measured protein concentration in mg/ml and *t* is the incubation time (30 min).

The mean value and its corresponding standard deviation was calculated with KaleidaGraph v4.1.3 and systematic errors from the protein concentration and the phosphate standard curve where incorporated in the final data. The calculated data were plotted against the $CuCl_2$ or ATP concentration and curve fitting was performed using a Michaelis-Menten enzyme kinetics reaction with KaleidaGraph v4.1.3 (2):

$$v = \frac{v_{max}[s]}{K_m + [s]} \quad (2)$$

Data statistics are reported with the mean value and the standard error. Physical outliers (negative absorption) have been removed from the curve fitting and the experimental measurement errors (σ_i) were used to weight particular experimental points in the data set.

Charge transfer measurements on solid supported membranes

E. coli membrane fragments, enriched with wtLpCopA and selected mutants, were prepared by the membrane isolation protocol previously described [1]. Thereafter, to remove loosely bound contaminant proteins from the membrane fraction the membranes were suspended (15 mL/g) in washing buffer containing 20 mM Tris-HCl pH=7.6, 1500 mM KCl, 20% glycerol, 5 mM BME, 1 mM $MgCl_2$ and 0.1 mg/mL $C_{12}E_8$. The membranes were then isolated by ultracentrifugation at 250000 xg for 5 hours and resuspended (15 mL/g) in 20 mM Tris-HCl pH=7.6, 200 mM KCl, 20% glycerol, 5 mM BME and 1 mM $MgCl_2$. LpCopA bands were quantified on a SDS-PAGE gel using the software ImageJ. Subsequently, the LpCopA concentrations in the different samples were equalize by dilution in suspension buffer.

The membrane fragments were adsorbed on an SSM during an incubation time of 60 minutes. The SSM consists of an alkanethiol monolayer covalently bound to a gold electrode via the sulfur atom, and further coated with a phospholipid monolayer. Following adsorption, wtLpCopA or mutants were activated by an ATP concentration jump. If the ATP jump induces a net charge movement within the protein, a current transient is recorded due to the capacitive coupling between membrane fragment and SSM [4, 5]. The method allows electrogenic steps of the first catalytic cycle to be detected, and is not sensitive to steady-state currents [4, 5].

The buffer solution contained 150mM NaCl, 5mM KCl, 5mM $MgCl_2$, 40mM MOPS, pH 6.8 (KOH), 5mM NaN_3, 20mM cysteine, and 0.5mM $CuCl_2$ or 10μM ammonium-tetrathiomolybdate (TTM) (as copper chelator). ATPase activation was obtained by rapidly exchanging the buffer solution with an identical buffer solution containing 100μM ATP.

The concentration jump experiments were carried out by employing the SURFE^{2}R^{One} device (Nanion Technologies, Munich, Germany). The temperature was maintained at 22-23 °C for all the experiments.

Each measurement was repeated 6 times (two minute waiting time after each measurement) and averaged to improve the signal to noise ratio. Standard deviations did not exceed 5%. Moreover, each set of measurements was typically reproduced using 2-3 different SSM electrodes.

References

1. Gourdon P, Liu X-Y, Skjørringe T, Morth JP, Møller LB, Pedersen BP, Nissen P (2011) Crystal structure of a copper-transporting PIB-type ATPase. *Nature* **475:** 59-64
2. Ankudinov AL, Ravel B, Rehr JJ, Conradson SD (1998) Real-space multiple-scattering calculation and interpretation of x-ray-absorption near-edge structure. *Phys Rev B* **58:** 7565-7576
3. Cariani L (2004) Bismuth citrate in the quantification of inorganic phosphate and its utility in the determination of membrane-bound phosphatases. *Anal Biochem* **324:** 79-83
4. Lewis D, Pilankatta R, Inesi G, Bartolommei G, Moncelli MR, Tadini-Buoninsegni F (2012) Distinctive Features of Catalytic and Transport Mechanisms in Mammalian Sarco-endoplasmic Reticulum Ca^{2+} ATPase (SERCA) and Cu^{+} (ATP7A/B) ATPases. *J Biol Chem* **287:** 32717-32727
5. Tadini-Buoninsegni F, Bartolommei G, Moncelli MR, Pilankatta R, Lewis D, Inesi G (2010) ATP dependent charge movement in ATP7B Cu^{+}-ATPase is demonstrated by pre-steady state electrical measurements. *FEBS Lett* **584:** 4619-4622
6. Robert X, Gouet P (2014) Deciphering key features in protein structures with the new ENDscript server. *Nucleic Acids Res* **42:** W320-324

Supplementary Figures

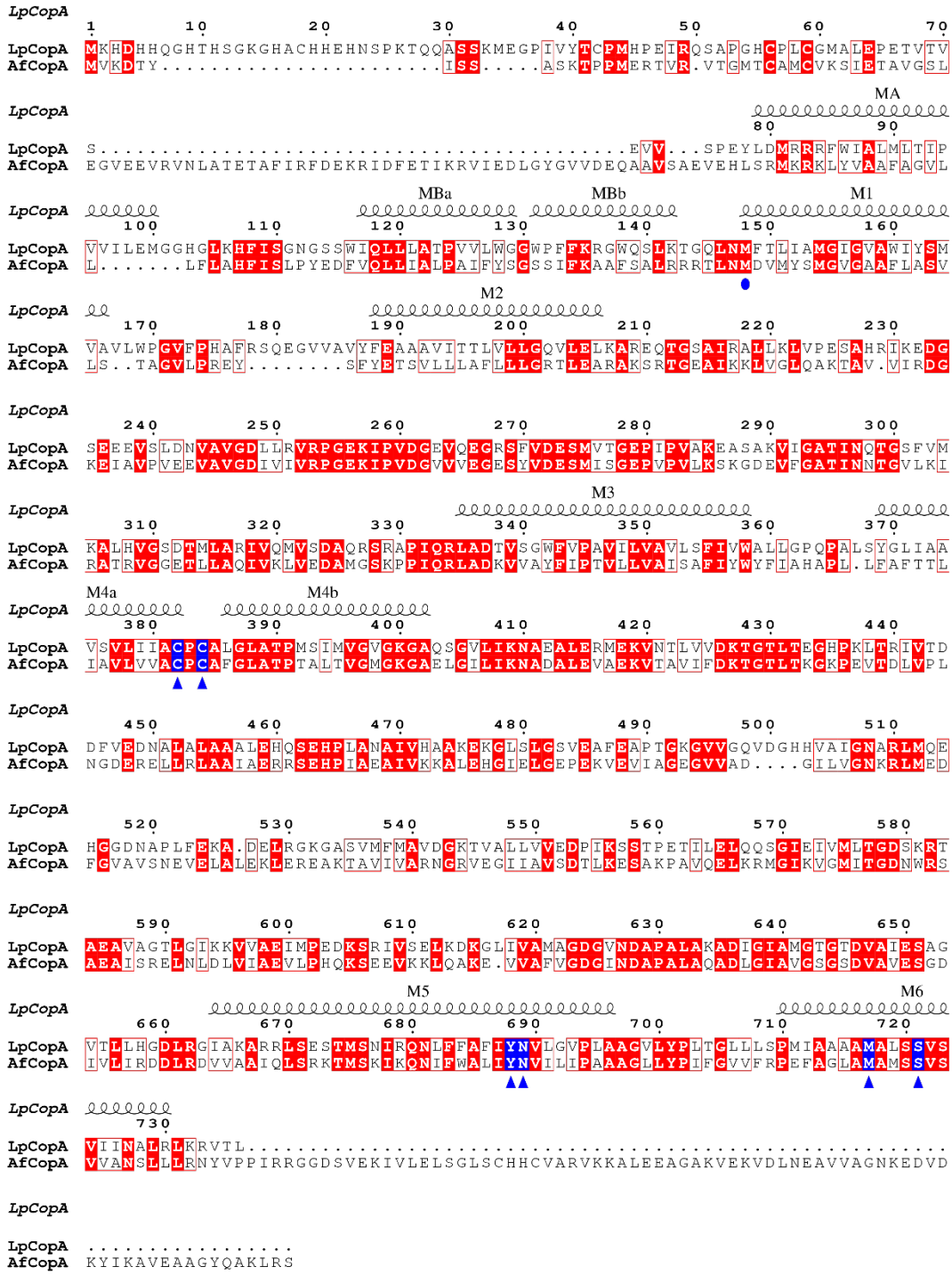

Supplementary Figure 1 Sequence alignment between *Legionella Pneumophila* CopA and *Archaeoglobus Fulgidus* CopA.

The conserved residues are highlighted in red and similar residues in red boxes.
The proposed TM metal binding residues discussed in the text are highlighted by blue arrows, while the conserve “entry-site” methionine by a blue circle. The figure has been generated with Espript 3.0 [6].

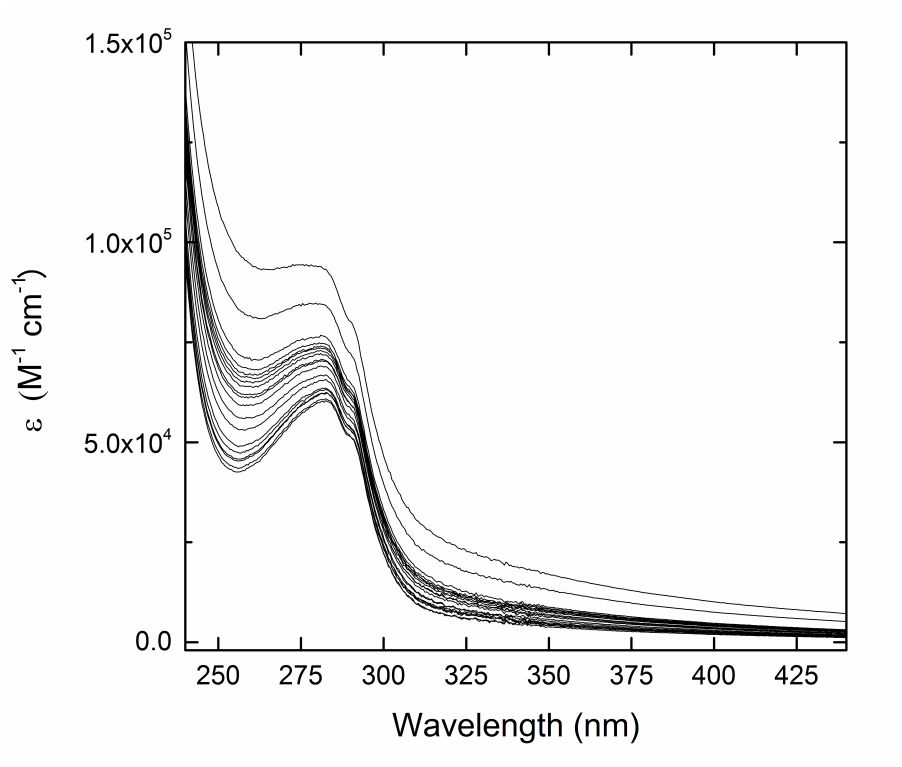

Supplementary Figure 2: Electronic absorption (UV-Vis) spectra of LpCopA titrated with Cu^+.

$[Cu(CH_3CN)_4]PF_6$ (0.25 eq. until 4 eq./LpCopA was reached, afterwards 1 eq./LpCopA until 6 eq./LpCopA) was titrated to the wild-type LpCopA (5.5 µM) and a spectral scan was recorded after each titration on a Varian Cary UV-Vis spectrophotometer. A metal-induced transitions envelope centered around 240-260 nm overlaying backbone and aromatic residues contributions occurred at low Cu-LpCopA ratios (<3-4) in agreement with formation of CysS-Cu^+ ligands-to-metal charge transfer transitions. However this was followed by increasing light scattering (as monitored at 420 mm) when 4-6 equivalents of Cu^+ were added to the wild-type LpCopA indicating the susceptibility to erroneous Cu^+ binding and consequent aggregation in absence of weak chelators. A small absorbance jump due to source changeover at 340 nm has been corrected.

Similar indications were obtained upon Cu^+ to protein stoichiometry determinations conducted upon titration of LpCopA followed by size-exclusion and Cu^+ quantification by ICP-MS. The amount of copper bound was significantly higher than the expected binding sites anticipated by the available crystal structure as well from binding based on AfCopA studies. We

reasoned that LpCopA is sensitive to precipitation in absence of chelators and the complete set of experiments was thus performed in the presence of cysteine.

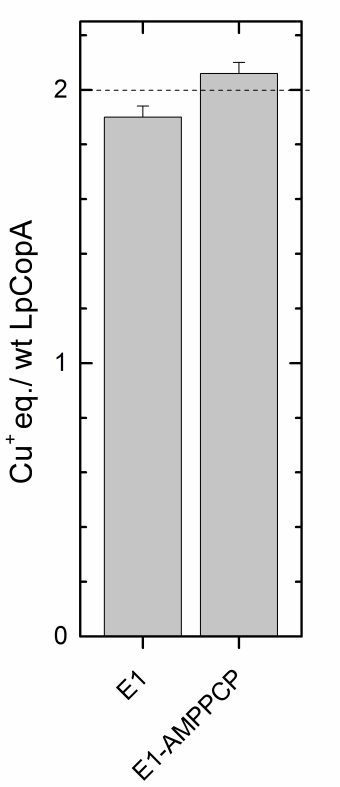

Supplementary Figure 3: Determination of Cu^+-binding stoichiometry in wtLpCopA and its nucleotide-analogue (AMPPCP) bound state by inductively coupled plasma mass-spectrometry.

The wtLpCopA was incubated with Cu^+ as described in the Material and Methods section. Additionally 1 mM nucleotide analogue was added. Cu^+-binding stoichiometry was determined upon Cu^+ reconstitution of protein samples in anaerobic atmosphere and removal of metal excess by size-exclusion chromatography. Protein concentrations were determined by Bradford method and Cu^+ content by ICP-MS.

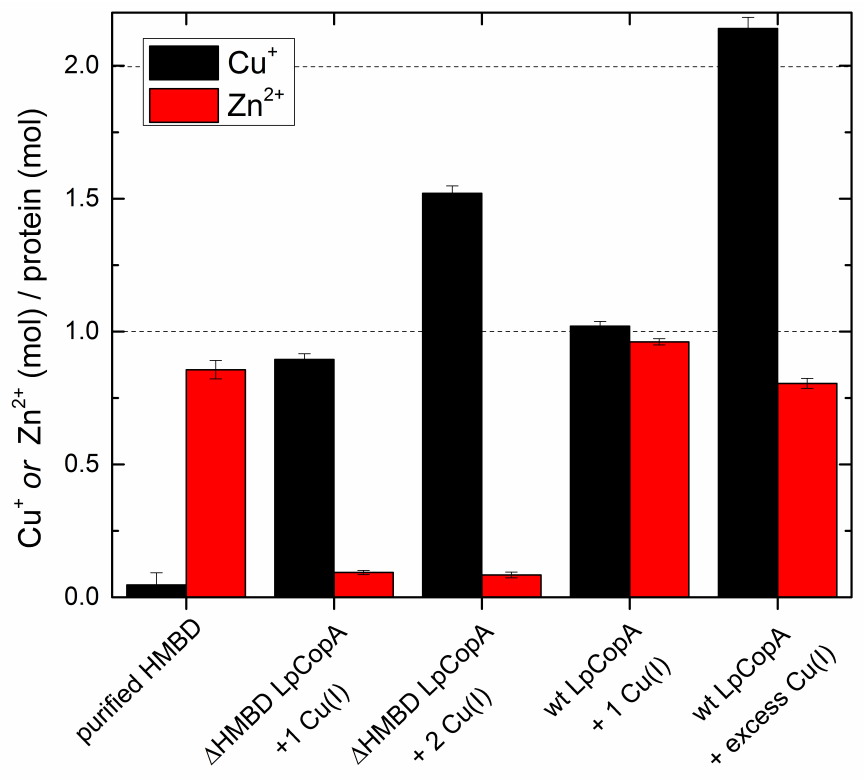

Supplementary Figure 4: Determination of Cu^{+}- and Zn^{2+}- binding stoichiometry in wtLpCopA and ΔHMBDLpCopA (XAS samples) compared to purified N-terminal HMBD.

Protein concentrations were determined by absorption of their aromatic residues at 280 nm and Cu^{+} and Zn^{2+} content by ICP-MS.

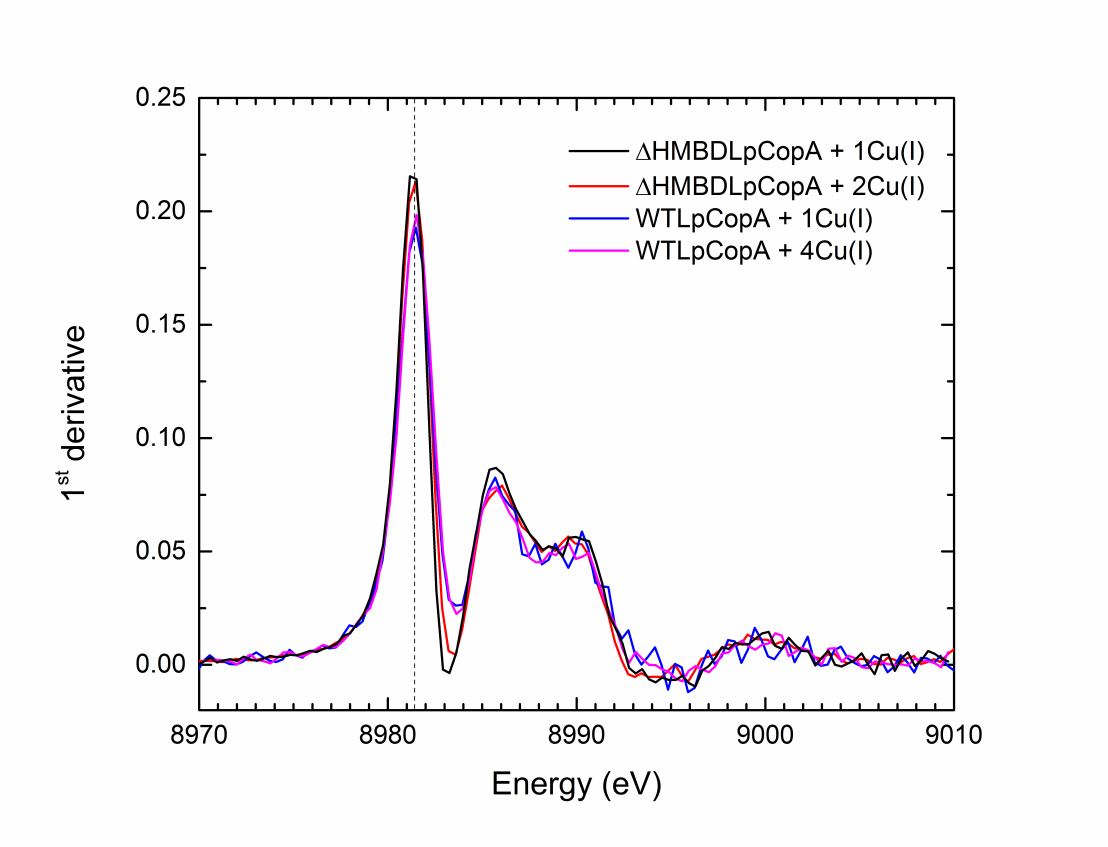

Supplementary Figure 5: First derivative of the XANES spectra of LpCopA- Cu^{+}.

The first derivative of the XANES spectra of ΔHMBDCopA-Cu^{+} (Cu^{+}:protein 1:1 or 1:2) and wtLpCopA (Cu^{+}:protein 1:1 or 1:4) shows the first primary inflection points at essentially the same energy (~8981 eV, indicated by the dotted line) and intensity, in agreement with the presence of Cu^{+} sites with very similar coordination.

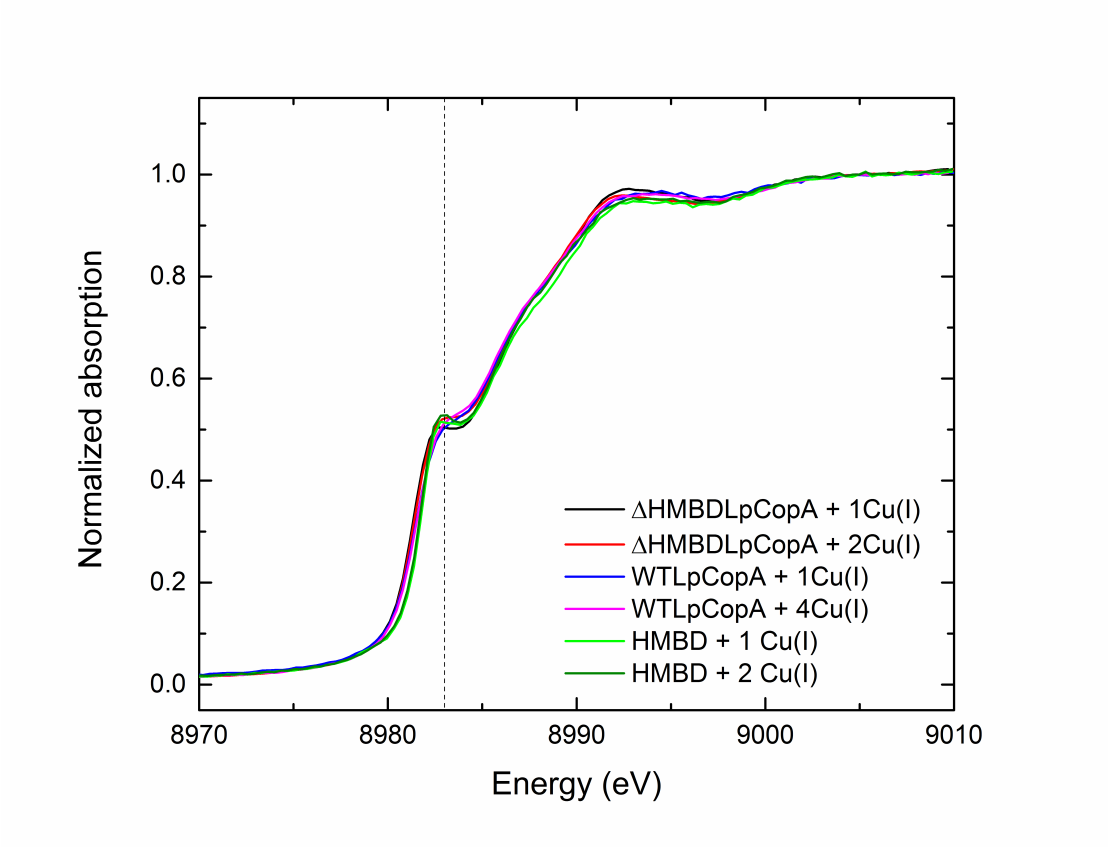

Supplementary Figure 6: XANES spectra of LpCopA-Cu^+, ΔHMBDCopA-Cu^+ and HMBD-Cu^+.

Normalized XANES spectra of wtLpCopA-Cu^+ (Cu^+:protein 1:1, blue line; Cu^+:protein 4:1, magenta line) and ΔHMBDCopA-Cu^+ (Cu^+:protein 1:1, black line; Cu^+:protein 2:1 red line) in 20 mM Tris-HCl pH=7.6, 200 mM KCl, 1 mM $MgCl_2$, 0.15 mg/ml $C_{12}E_8$, 20% glycerol. These spectra are compared to the normalized XANES spectra of HMBD-Cu^+ (Cu^+:protein stoichiometry 1:1, black line) and HMBD-Cu^+ (Cu^+:protein 2:1, red line) in 50 mM Tris-HCl, 250 mM NaCl pH=8. The peak position of the 1s→4p transition at 8983 eV is indicated by the dotted line.

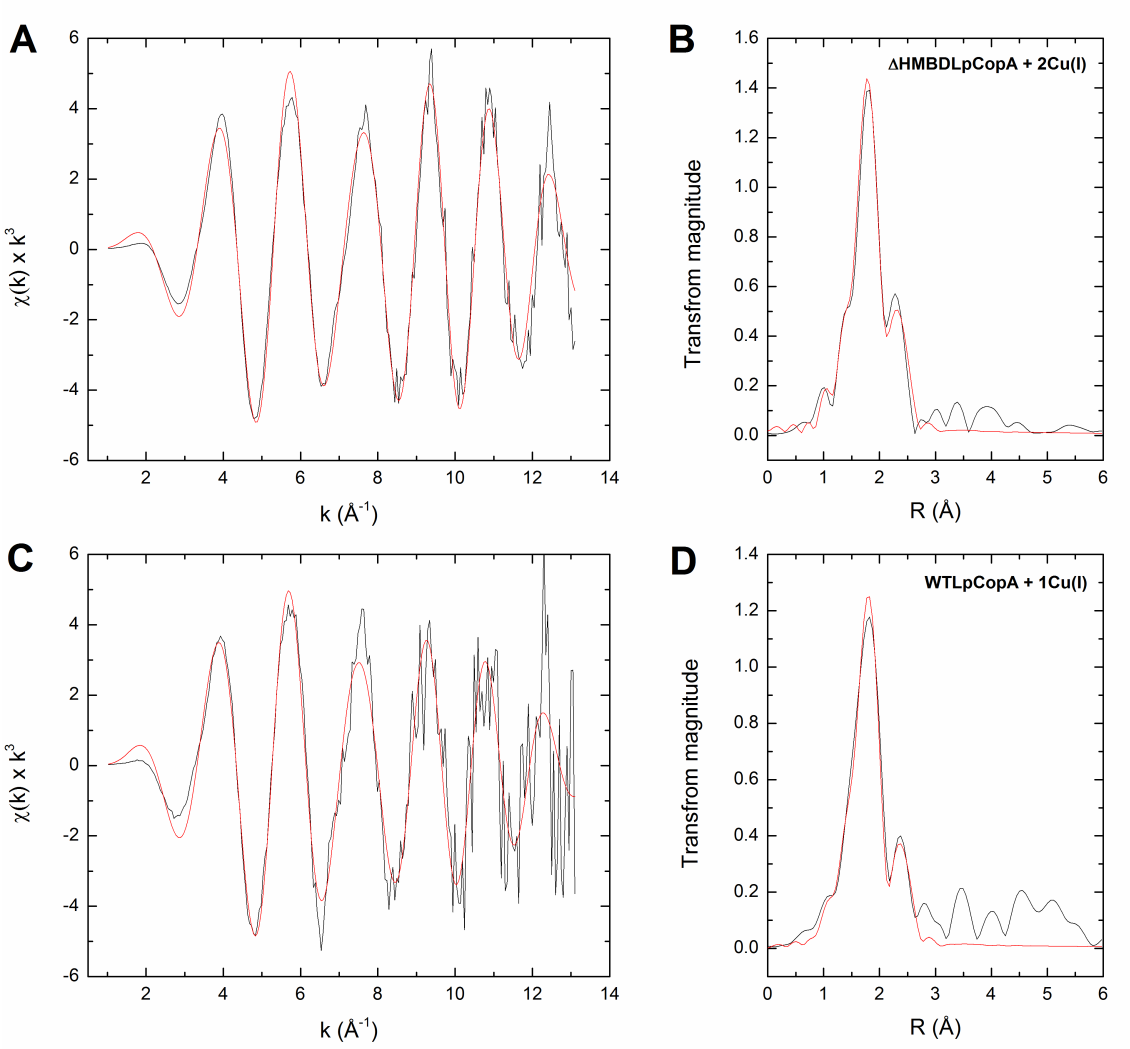

Supplementary Figure 7: Cu K-edge EXAFS and Fourier transforms of ΔHMBDCopA and wtLpCopA.

Experimental EXAFS data (black line) and best fits (red line) (A,C), and the corresponding Fourier transforms (B,D) for saturated ΔHMBDCopA-Cu^+ (A) (Cu^+:protein stoichiometry 2:1), and wtLpCopA-Cu^+ (Cu^+:protein stoichiometry 1:1) (C) in 20 mM Tris-HCl pH=7.6, 200 mM KCl, 1 mM $MgCl_2$, 0.15 mg/ml $C_{12}E_8$, 20 %(w/v) glycerol. The parameters for the best fits are listed in Table II.

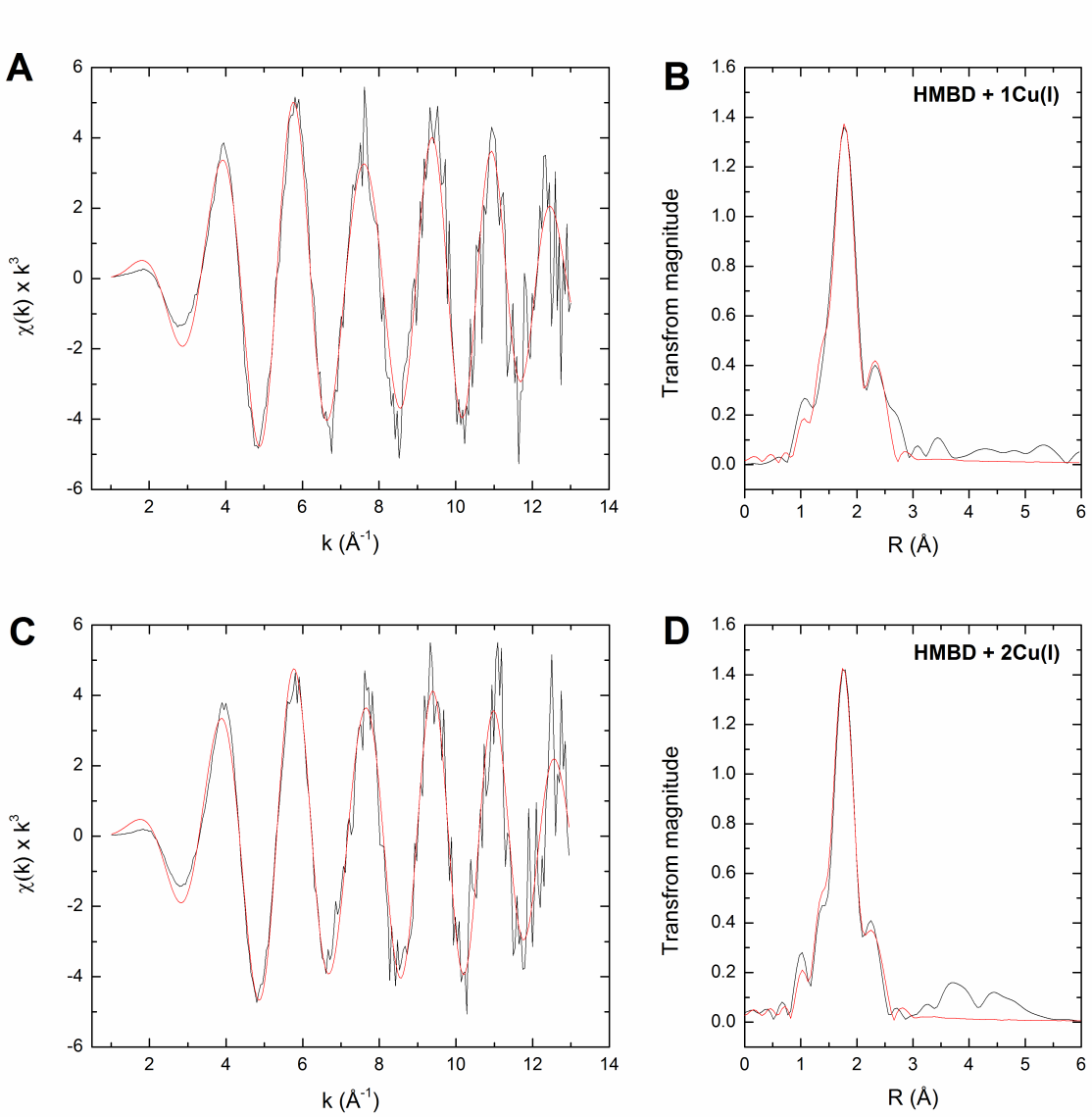

Supplementary Figure 8: Cu^+ K-edge EXAFS and corresponding Fourier transforms of HMBD of LpCopA.

Experimental EXAFS data (black line) and best fits (red line) (A,C), and corresponding Fourier transforms (B,D) for HMBD-Cu^+ (Cu^+:protein stoichiometry 1:1) (A) and HMBD-Cu^+ (Cu^+:protein stoichiometry 2:1) (C) in 50 mM Tris-HCl, 250 mM NaCl pH=8. The parameters for the best fits are listed in Supplementary Table II.

Supplementary Table I: Extended X-ray absorption fine structure (EXAFS) curve-fitting results for ΔHMBDLpCopA.

Protein	Cu^+ eq. added	Scattering Paths	N	R (Å)	σ^2 ($Å^2$)	F
ΔHMBD LpCopA	1	Cu-S	2	2.249(4)	0.0030(4)	0.298
		Cu-S	1	2.270(4)	0.009(3)	
		Cu···Cu	1	2.707(6)	0.0051(4)	
		Cu-S	2	2.263(4)	0.0024(2)	0.305
		Cu-N/O	1	2.060(2)	0.003(1)	
		Cu···Cu	1	2.712(5)	0.0056(4)	
		Cu-S	1	2.293(6)	0.0014(5)[1]	0.332
		Cu-N/O	2	2.116(5)	0.0009(5)[1]	
		Cu···Cu	1	2.741(6)	0.0057(5)	
	2	Cu-S	2	2.228(4)	0.0075(1)	0.192
		Cu-S	1	2.262(3)	0.005(2)	
		Cu···Cu	1	2.702(3)	0.0069(3)	
		Cu-S	2	2.261(2)	0.0020(1)	0.197
		Cu-N/O	1	2.030(1)	0.005(1)	
		Cu···Cu	1	2.711(4)	0.0072(4)	
		Cu-S	1	2.290(4)	0.0015(3)[1]	0.254
		Cu-N/O	2	2.125(3)	0.0010(4)[1]	
		Cu···Cu	1	2.746(5)	0.0078(5)	

Coordination numbers are indicated by N, interatomic distances R are given in Å (the values in parentheses are the estimated standard deviations), Debye-Waller factors σ^2 (the mean-square deviations in interatomic distance, the values in parentheses are the estimated standard deviations) in $Å^2$, and the fit-error function F is defined by $F = \sqrt{\sum k^6(\chi(k)_{calcd} - \chi(k)_{exp})^2 / \sum k^6 \chi(k)_{exp}^2}$ where $\chi(k)$ are the EXAFS oscillations and k is the photo-electron wave number.

[1] The Debye-Waller factors have been linked in the fitting to prevent free floating of Cu-S to negative values.

Supplementary Table II: Extended X-ray absorption fine structure (EXAFS) fitting results for HMBD-Cu^{+}.

Protein	Cu^{+} eq. added	Scattering Paths	N	R (Å)	σ^2 ($Å^2$)	F
HMBD	1	Cu-S	3	2.249(3)	0.0047(2)	0.363
		Cu···Cu	1	2.682(7)	0.0071(7)	
	2	Cu-S	3	2.237(3)	0.0044(1)	0.320
		Cu···Cu	1	2.654(7)	0.0081(7)	

Coordination numbers are indicated by N, interatomic distances R are given in Å, Debye-Waller factors σ^2 (the mean-square deviations in interatomic distance) in $Å^2$, and the fit-error function F is defined by $F = \sqrt{\sum k^6(\chi(k)_{calcd} - \chi(k)_{exp})^2 / \sum k^6 \chi(k)_{exp}^2}$ where $\chi(k)$ are the EXAFS oscillations and k is the photo-electron wave number. The values in parentheses are the estimated standard deviations.

Supplementary Table III: ATPase activity by LpCopA and mutants determined as a function of Cu^{+} concentration.

	$K_{1/2,Cu}$ (mM)	v_{max} (nmol mg^{-1} min^{-1})	Fitting (R)
wt LpCopA	0.0006 ± 0.0002	19.8 ± 0.7	0.97
ΔHMBD LpCopA	0.11 ± 0.02	5.7 ± 0.3	0.96
LpCopA D426N	(1.6 ± 1.1)	2.6 ± 1.0	0.97
LpCopA C18S C42S C56S C59S	(0.5 ± 2.4)	3 ± 6[1]	0.89
LpCopA M148V	(0.008 ± 0.004)	1.2 ± 0.1[1]	0.93
LpCopA C382S C384S	(0.16 ± 0.05)	2.2 ± 0.2[1]	0.99
LpCopA C382S C384S M717A	(0.7 ± 0.2)	1.6 ± 0.2[1]	0.98

[1] Data are comparable to D426N. Residual activity is not accurately measurable.

Supplementary Table IV: ATPase activity by LpCopA and mutants determined as a function of ATP concentrations.

	$K_{1/2,ATP}$ (mM)	v_{max} (nmol mg^{-1} min^{-1})	Fitting (R)
wt	0.29 ± 0.02	17.5 ± 0.4	1.0
ΔHMBD	0.59 ± 0.04	7.1 ± 0.1	0.96
D426N	(5.5 ± 1.6)	3.9 ± 0.6	0.94
C18S C42S C56S C59S	(0.26 ± 0.04)	5.7 ± 0.2[2]	0.96
M148V	(0.7 ± 0.2)	5.9 ± 0.7[2]	0.98
C382S C384S[1]	(2.2 ± 1.7)	3 ± 1[2]	0.89
C382S C384S M717A	(7.7 ± 2.9)	5.3 ± 1.3[2]	0.98

[1] Data are not weighted according to their experimental error.

[2] Data are comparable to D426N. Residual activity is not accurately measurable.